JOURNAL OF MATERIALS SCIENCE 32 (1997) 6141–6146

Evaluation of thermal recovery of neutron-irradiated SA508-3 steel using magnetic property measurements

DUCK-GUN PARK, JUN-HWA HONG
Reactor Materials Department, Korea Atomic Energy Research Institute, Daeduk, Taejon 305-353, South Korea

IN-SUP KIM, H. C. KIM*
*Departments of Nuclear Engineering, and *Physics, Korea Advanced Institute of Science and Technology, Daeduk, Taejon 305-701, South Korea*

The Vickers microhardness and magnetic properties have been used to investigate irradiation effects and thermal recovery characteristics of neutron-irradiated SA508-3 reactor pressure vessel steel specimens irradiated to a neutron fluence of 5.5×10^{17} n cm^{-2} ($E > 1$ MeV) at 70 °C. Two recovery stages were identified from the hardness results during isochronal annealing and the mechanism responsible for the two stages was explained using the results of Barkhausen noise on the basis of the interaction between radiation-induced defects and the magnetic domain wall. The neutron irradiation caused the coercivity to decrease, whereas the maximum magnetic induction increased. Barkhausen noise parameters associated with the domain-wall motion were decreased by neutron irradiation and recovered with subsequent heat treatments. From the sensitive changes in the Barkhausen noise upon annealing heat treatment, it is suggested that the Barkhausen noise measurements may be used as a useful tool for monitoring the early stage of the thermal recovery behaviour of neutron-irradiated reactor pressure vessel steels.

1. Introduction

Among various mechanical and physical techniques, the magnetic methods have been shown to have the potential to detect radiation hardening and embrittlement in reactor pressure vessel (RPV) steel [1]. The deterioration in the mechanical properties due to neutron irradiation and recovery by thermal annealing has been explained in terms of interaction between dislocation and defect clusters such as vacancies, vacancy–impurity complexes or fine precipitates [2, 3]. However, the underlying mechanism responsible for the change in magnetic properties after irradiation is not understood yet. Nonetheless, these defects are expected to affect the change in the magnetic properties to some extent by strong interaction with the domain walls analogous to that of small precipitates with a spontaneous magnetization different from that of the matrix [4].

The hardness change in the irradiated specimens due to isochronal and isothermal heat treatments has been used as a measure of the radiation damage mechanism associated with defect dynamics involving stability, mobility and mutual interaction of defects produced during irradiation [5]. In the present work, irradiation effects and thermal recovery characteristics of neutron-irradiated RPV steel were investigated using hardness and magnetic measurements and the results were analysed on the basis of radiation damage mechanism and ferromagnetic domain theory.

2. Experimental procedure

2.1. Material and neutron irradiation

The specimens used in the present study were SA508-3 forged steel for nuclear pressure vessel produced by Korea Heavy Industries and Construction Co, and the chemical composition is shown in Table I.

Specimens were irradiated for 9 months for 8 h a day for several cycles at full power of 1.5 MW in the Triga Mark III reactor of the Korea Atomic Energy Research Institute. The total accumulated fluence determined by iron was 5.5×10^{17} n cm^{-2} ($E > 1$ MeV). The irradiation temperature determined by low-melting eutectic materials was approximately 70 °C.

2.2. Thermal annealing and microhardness measurements

The specimens were annealed in a small bath containing a silicone oil with a temperature of up to 300 °C and in a salt ($NaNO_3 : KNO_3 = 50 : 50$) bath. The

0022–2461

TABLE I Chemical composition and heat treatment of SA508-3 steel which had the following heat treatment history: 1133–1153 K for 4.5 h water quenching; 928–933 K for 9 h air cooling; 92 K for 24 h air cooling (simulated post weld heat treatment)

Element	C	Si	Mn	P	S	Ni	Cr	Mo	Al	Cu	V	Co	As	Fe
Amount (wt%)	0.17	0.004	1.42	0.004	0.003	0.98	0.22	0.58	0.003	0.045	0.003	0.006	62 ppm	Balance

furnace temperature was raised to a predetermined annealing temperature and held constant for 1 h using a proportional integral differential PID controller. The specimen temperature was monitored with a thermocouple fixed at the bottom of the bath where specimens were located. The specimen was withdrawn from the bath after a predetermined annealing time and cooled to room temperature.

The isochronal annealing was performed from 150 to 525 °C with 40 min of constant annealing time during each step and a temperature interval of 15–35 °C. The isothermal annealing was carried out at 362 and 474 °C, where two distinctive recovery stages were revealed in the isochronal annealing and continued until the asymptote appeared.

The Vickers microhardness measurement was conducted to assess the recovery of radiation damage following the ASME Standard E-384, "Standard test methods for microhardness of materials". The test load and time duration were 200 g and 15 s, respectively, and the tests were conducted about 15–25 times.

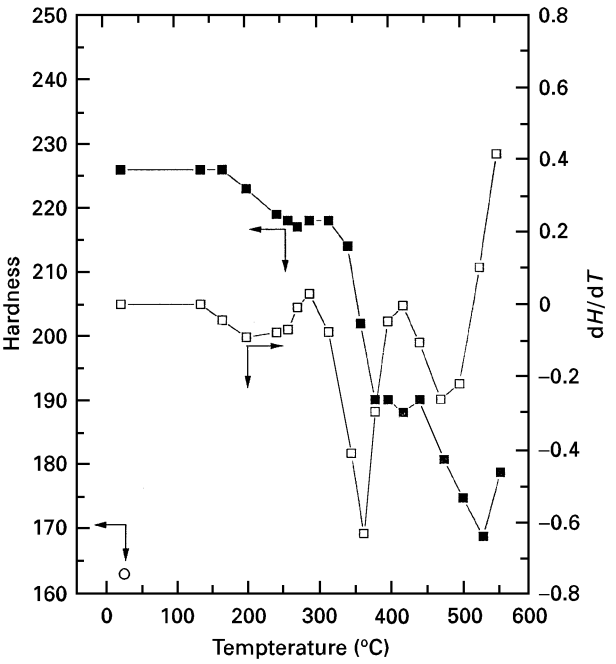

Figure 1 Integral (■) and differential (□) isochronal annealing curves of neutron-irradiated SA508-3 steel. (○), unirradiated steel.

2.3. Magnetic properties

Specimens in the shape of cylindrical pins with a diameter of 1.5 mm and a length of 15 mm were magnetized using a specially designed yoke magnet with an amplified sinusoidal wave current of 0.1 Hz. The maximum current intensity was set sufficiently high to extend the hysteresis loop beyond the range of approach to saturation. The magnetic hysteresis loop (B–H) was measured with a fluxmeter and a gaussmeter and the data were stored in an IBM personal computer connected to the storage oscilloscope. The stored data were processed by analysis software and Barkhausen noise for a half-cycle of magnetization, Barkhausen parameters above the threshold amplitude of 0.2 V were calculated.

3. Results and discussion

3.1. Radiation hardening and recovery

3.1.1. Isochronal annealing

The variation in Vickers hardness after isochronal annealing is shown in Fig. 1, where both the integral and the differential recovery curves are presented as functions of annealing temperature.

The recovery takes place in two annealing stages in the isochronal annealing: stage I at around 362 °C and stage II at around 474 °C. These were confirmed in the differential isochronal annealing curve as seen in Fig. 1. The annealing effectiveness indicated by the decrease in the hardness increased with increasing annealing temperature in agreement with other studies [6, 7]. The contributions of the recovery stages to the total recovery were approximately 57% and 33% for stage I and stage II, respectively. The remaining 10% was unrecovered even after 40 min at 520 °C.

Most of the induced self-interstitials are annealed out at dislocations by irradiation at the ambient temperature in the research or power reactor at around 70 °C [8]. At around this temperature the vacancies are expected to be immobile [9], and only vacancy clusters are produced during irradiation [5]. The impurity atoms migrate around and are trapped by immobile point defects, presumably vacancies. These vacancy–impurity complexes provide a stronger barrier to dislocation motion than the impurity alone in solution [10].

The hardness difference between unirradiated and irradiated specimens, $\Delta H_V = 63$, is very large considering the fluence level compared with that of 15 in the SA508-3 steel with dose of 9×10^{18} n cm^{-2} ($E >$ 1 MeV) at 290 °C [11]. It is known that the hardness decreases with increasing irradiation temperature [10] and the SA508-3 steel was fairly insensitive to higher irradiation temperatures [12]. The present results suggest that the degradation is more pronounced for irradiation at lower temperatures.

With regard to the defects size, the hardening is sensitive to defect diameters in the range 1–2 nm [13]. Small-angle neutron scattering results for SA508-3 steel irradiated at 290 °C revealed induced microvoids of 2–4 nm diameter and the defect sizes increased with

increasing irradiation temperature [11]. The large hardness change in this study also suggests that the size of vacancy clusters and/or vacancy–impurity complexes by neutron irradiation may be within this range. As the annealing proceeds, firstly the small vacancy clusters were annealed and the maximum void size increases as the void number density decreased [14]. Thus it can be said that the hardness recovery on isochronal annealing is attributed to the decrease in the concentration of vacancy clusters, resulting in the removal of dislocation barriers.

3.1.2. Isothermal annealing

The hardness changes due to isothermal annealing in SA508-3 steel at 362 and 474 °C are shown in Fig. 2. The microhardness decreased abruptly within 10 min and annealing recovery amounts were approximately 68% and 85% at 362 °C and 474 °C, respectively. The asymptote of the annealing curve appeared after 75 min at 362 °C and after 30 min at 474 °C. This annealing time is very short in comparison with that of the conventional recovery time of longer than 2 h (120 min), reported for low-alloy steel irradiated to a fluence of 10^{19} n cm^{-2} at 290 °C [6, 7].

It is generally accepted that the recovery of irradiation hardening is governed by a thermally activated process; thus the recovery activation energy is often used as an index to represent the recovery mechanism related with defect dynamics [6]. Small vacancy clusters of low activation energy dissolve away more rapidly than large vacancy clusters do [3] and the recovery activation energy of defect increases with increasing fluence and also with increasing irradiation time [10]. In this study, the fluence level is low and the irradiation time is very short in comparison with those in the power reactor; therefore the activation energy of defect clusters is expected to be small. The rapid radiation recovery in this study may be attributed to small defect clusters of low activation energy.

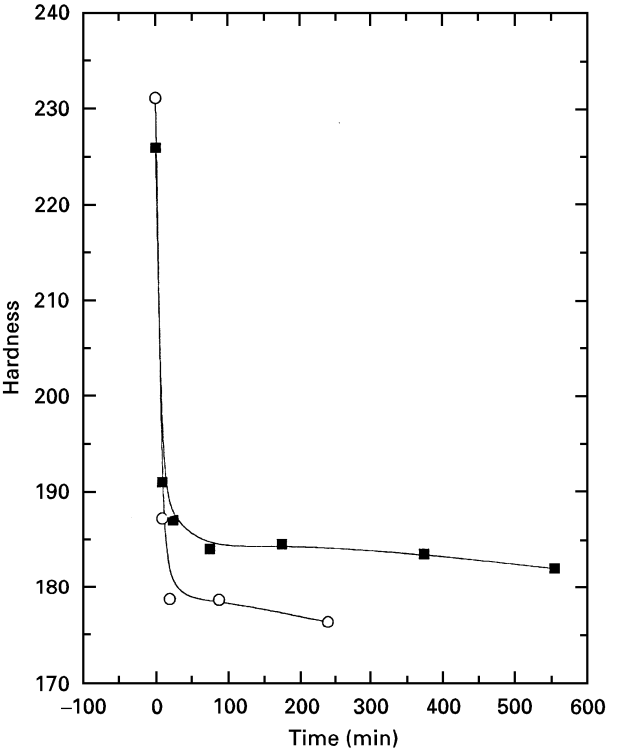

Figure 2 Isothermal recovery curve of neutron-irradiated SA508-3 steel measured by the Vickers microhardness. (■), 362 °C; (○), 474 °C.

The results suggests that the two recovery stages most probably are due to the annealing of vacancy clusters and the release of interstitial impurity from its traps.

3.2. Magnetic properties

3.2.1. Hysteresis loop

Fig. 3 shows a comparison of the hysteresis loop for a cylindrical pin specimen before and after irradiation. The maximum magnetic induction increased by 3.8%

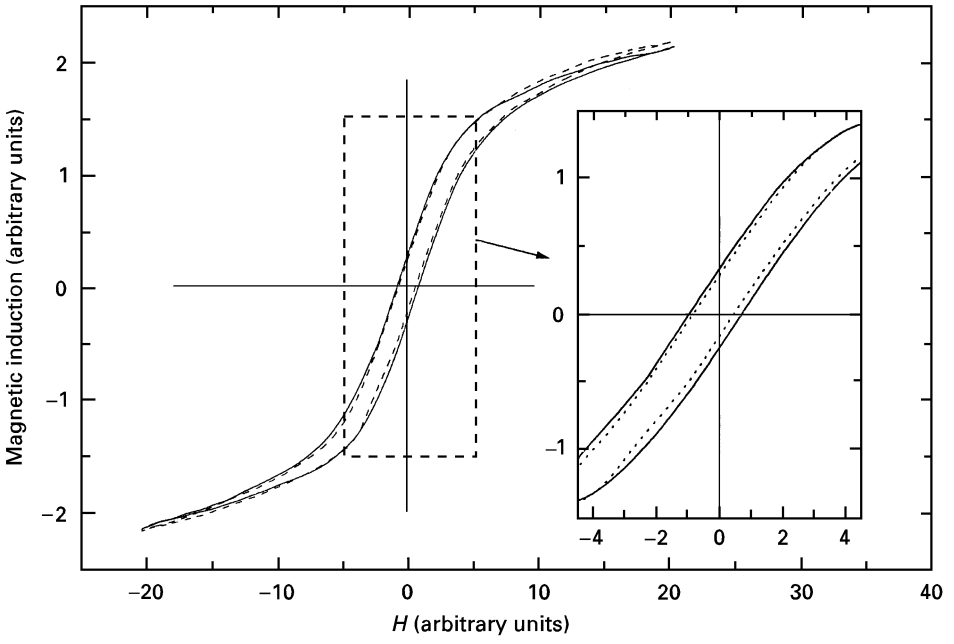

Figure 3 Typical hysteresis loop of unirradiated (——), and neutron-irradiated (– – –) SA508-3 steel.

but the coercivity decreased by 8.7% on irradiation, in agreement with the results of others [15].

The coercivity is the field required to move the wall and increases when the motion of domain walls is impeded by defects. Vacancy clusters within a domain wall tend to anchor the wall in order to decrease the area, and hence the energy of the wall. Consequently, the domain walls are attracted to the defects which effectively impede wall motion, leading to the increase in the coercivity of irradiated specimens [16]. These defects do not make a spike domain, because their magnetostatic energy is small [17].

Coercivity varies with the microstructural features characterizing specimen such as texture and atomic order depending on irradiation conditions. The specimens used in this experiment have a preferred orientation of transverse–longitudinal direction; defect alignments seem to have occurred along a preferred direction via radiation-enhanced diffusion as a result of neutron irradiation. The defect alignments along the preferred orientation may give rise to an increase in magnetic anisotropy energy. The decrease in coercivity in the present specimen may arise from compensation of wall energy by increasing the anisotropy energy.

The saturation magnetization is known to be insensitive to structure in the sense that it does not depend on the details of fine structure, such as strain, lattice imperfection or small amounts of impurities [17]. The maximum magnetic induction is proportional to the saturation magnetization for the same shape of specimen. Therefore, the microstructural change due to neutron irradiation would not cause any change in the maximum magnetic induction, in contrast with the observed results. The increase in maximum magnetic induction in this study associated with the decrease in wall energy induced by vacancy clusters.

3.2.2. Barkhausen noise

3.2.2.1. Barkhausen noise profile with isochronal annealing. The Barkhausen noise profiles during a half-cycle for the magnetization of unirradiated and neutron-irradiated specimens are shown in Fig. 4. The decrease in peak voltage in the Barkhausen envelope for the irradiated specimen is in agreement with the results of Sipahi *et al.* [18].

Fig. 5 shows the recovery of the Barkhausen noise count (BNC) for the irradiated specimen as a function of annealing temperature. The BNC, decreased by neutron irradiation, recovered by subsequent isothermal annealing and it is known that the BNC is proportional to the Barkhausen voltage [19]. The Barkhausen voltage decreases when the motion of the domain wall is impeded by a retarding force [20] and the vacancy clusters induced in the irradiated specimen act as a retarding barrier to wall displacement, decreasing the Barkhausen voltage at the coercive force.

In the course of thermal annealing, point defects and vacancies recombine, forming microvoids by the diffusion-controlled process. The concentration and surface area of a microvoid decrease by clustering with other vacancy clusters, resulting in a decrease in the ability of domain-wall pinning; thus the recovery of the BNC is accounted for by the decreased resistance to domain-wall motion.

3.2.2.2. Barkhausen noise change with isothermal annealing. Results of electron microscopy on neutron-irradiated iron showed that vacancy clusters grow and their density decreases, mainly in the range 300–400 °C [21], during which the concentration and surface area of the vacancy clusters are reduced, resulting in the recovery of the BNC.

The variation in the BNC as a function of annealing time at 362 °C and 474 °C is shown in Figs 6 and 7, respectively. The BNC recovered 95% within 3 min and then remained constant as shown in Fig. 6, where the BNC recovery ratio is defined as the BNC of the irradiated specimen to the BNC of the unirradiated specimen. The recovery rate of the BNC in the primary annealed specimen at 474 °C was lower than at 362 °C and decreased with increasing annealing time, contrary to expectation, since the recovery rate should increase with annealing temperature.

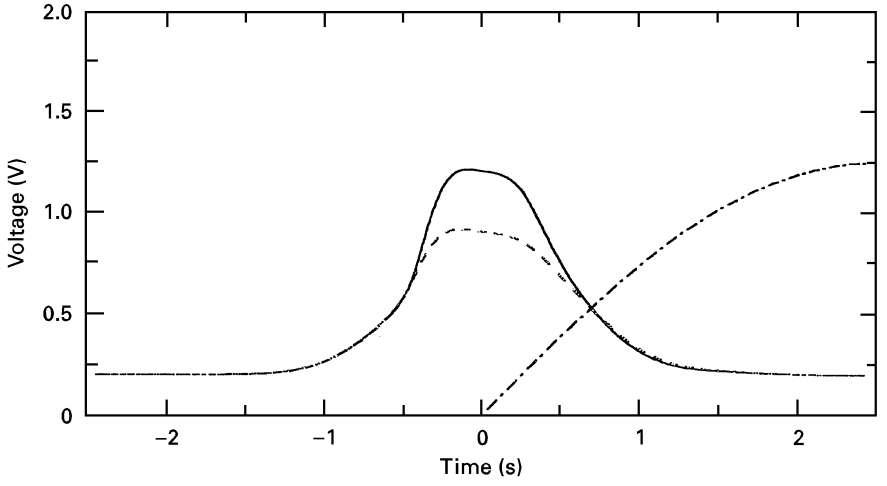

Figure 4 Barkhausen emission profile of unirradiated (——) and neutron-irradiated (– – –) SA508-3 steel (magnetizing frequency, 0.1 Hz). (—·—), induced field.

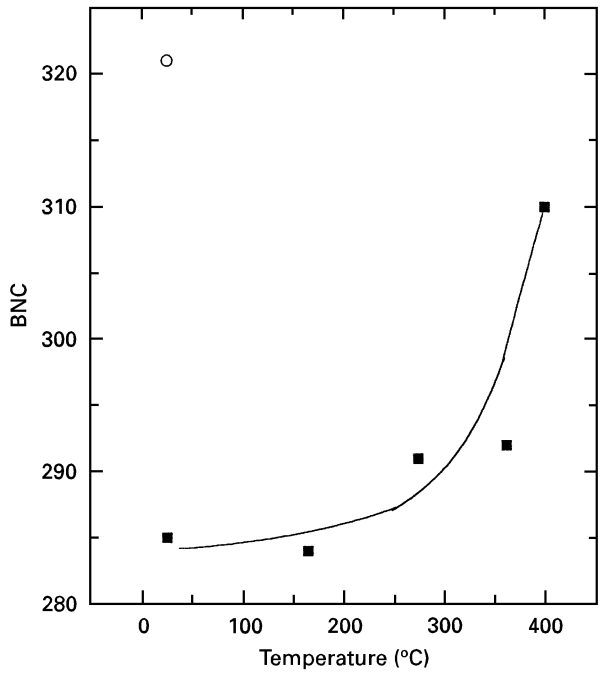

Figure 5 BNC as a function of annealing temperature (annealing time, 40 min). (○), unirradiated; (■), irradiated.

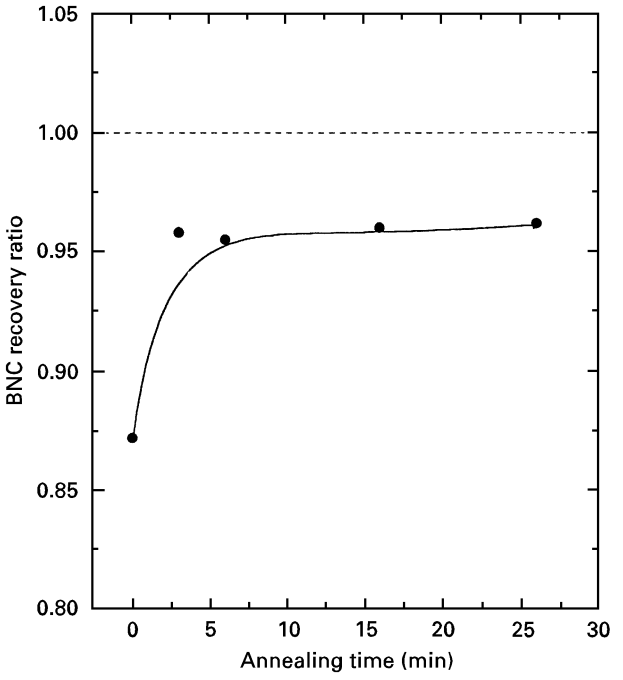

Figure 6 BNC recovery curve as a function of annealing time (annealing temperature, 362 °C).

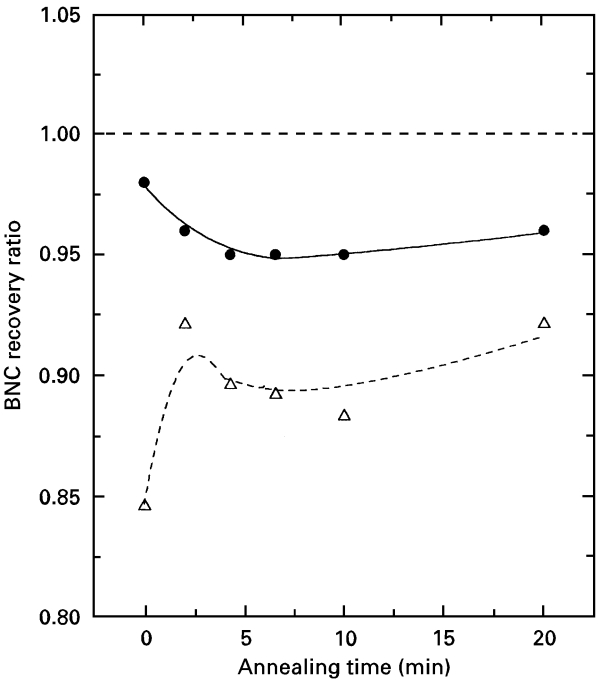

Figure 7 BNC recovery curve as a function of annealing time (annealing temperature, 474 °C). (△), primary annealing at 474 °C; (●), reannealing at 474 °C after an annealing at 362 °C.

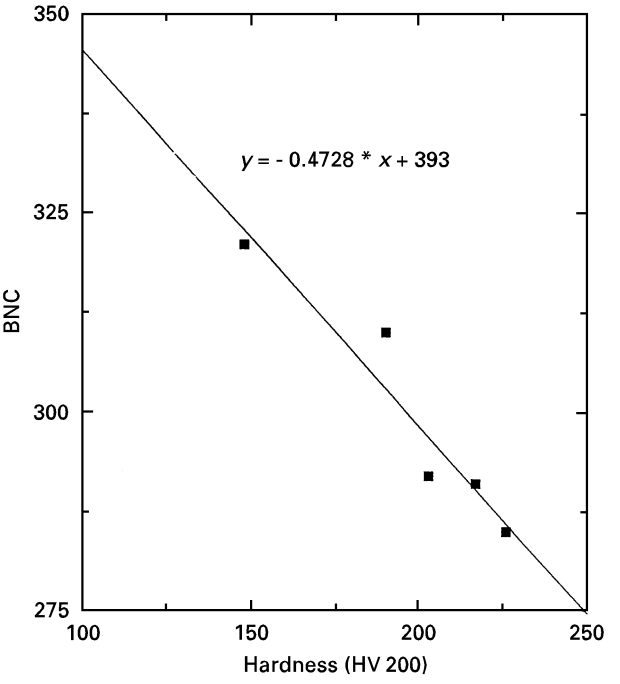

Figure 8 Correlation between BNC and the Vickers microhardness.

The recovery behaviour of the BNC in the primary annealed specimens at 474 °C seems to be attributed to the retardation of domain wall movement by decomposed vacancy–impurity complexes [22].

The initial high recovery rate of the BNC for the reannealed specimen at 474 °C can be explained in terms of the removal of the domain-wall barrier by the annealing of vacancy clusters. The following decrease in recovery rate is the consequence of the strengthening of these barriers to wall motion by the decomposed vacancy–impurity complexes. Therefore, it can be concluded that the decomposition of vacancy–impurity complexes arises at 474 °C because of the isothermal annealing and not at 362 °C because the binding energy of vacancy–impurity is larger than the vacancy migration energy [2].

3.3. Correlation between hardness and Barkhausen noise

Fig. 8 shows the relationship between the BNC and hardness after isochronal annealing where it gives some insight into the relation between mechanical and magnetic properties. The average correlation factor

for this parameter was 0.96. It shows good correlation, and a similar relationship between BNC and hardness was obtained by others [20]. Radiation hardening depends on the number of small vacancy clusters and/or vacancy–impurity complexes, whereas the recovery of BNC associated with the ability of domain-wall pinning depends on their concentration and surface area; thus good correlation is found. The empirical equation between BNC and Vickers microhardness is

$$\text{BNC} = -0.475 \times \text{hardness} + 393$$

The result suggests that the radiation hardening can be evaluated non-destructively by using Barkhausen noise parameters.

4. Conclusions

The present investigation of irradiation effects and thermal recovery characteristics in neutron-irradiated pressure vessel steel using hardness and magnetic properties yielded the following conclusions.

1. The irradiation hardening and recovery are attributed to vacancy clusters and vacancy–impurity complexes.

2. The decrease in coercivity in the irradiated specimen is attributed to the increase in magnetic anisotropy induced by the alignment of defects along a preferred orientation, and the increase in the maximum magnetic induction could be understood in terms of the decrease in the domain-wall energy.

3. The decrease in BNC in the irradiated specimen is interpreted as a hindrance to domain-wall motion induced by defects clusters, and the recovery of BNC due to heat treatment may be a result of the removal of the wall barrier by the annealing of defect clusters. From the analysis of annealing data of hardness and BNC data of post annealing, the first recovery stage seems to occur by annealing of vacancy clusters and the second stage by the decomposition of vacancy–impurity complexes.

4. The relationship between BNC and Vickers microhardness is given empirically as $\text{BNC} = -0.475 \times \text{hardness} + 393$, which suggests that the change in mechanical properties, like the hardness associated with radiation hardening, is evaluated non-destructively by using magnetic techniques of Barkhausen noise measurement.

References

1. W.-J. SHONG, J. F. STUBBINS and J. G. WILLIAMS, "Reactor Dosimetry", ASTM Special Technical Publication 1228 (American Society for Testing and Materials, Philadelphia, PA, 1994) p. 215.
2. R. A. JOHNSON and A. N. ORLOV, "Physics of radiation effects in crystals," Modern Problems in Condensed Matter Sciences, Vol. 13 (Elsevier, Amsterdam, 1986).
3. C. C. DOLLINS, *Radiat. Effects* **16** (1972) 271.
4. D. G. PARK, C. G. KIM, H. C. KIM, J. H. HONG and I. S. KIM, *J. Appl. Phys.*, **81**(8), 15 (1997) 4125.
5. W. SCHILLING, G. BURGER, K. ISEBECK and WENZL, "Vacancies and interstitials in metals" (North-Holland, Amsterdam, 1969).
6. D. PACHUR, "Effects of radiation on materials", ASTM Special Technical Publication 725 (American Society for Testing and Materials, Philadelphia, PA, 1981) p. 5.
7. S.-H. CHI and I.-S. KIM, *J. Nucl. Mater.* **230** (1966) 41.
8. M. E. DOWNEY and B. L. EYRE, *Phil. Mag.* Vol. 11, no. 109 (1964) 53.
9. R. A. JOHNSON, *Phys. Rev.* **134** (1964) A1329.
10. C. J. McHARGUE, *Int. Metall. Rev.* **27** (1982) 121.
11. J. T. BUSWELL, W. J. PHYTHIAN, R. J. McELORY, S. DUMBILL and P. H. N. RAY, *J. Nucl. Mater.* **225** (1995) 196.
12. G. R. ODETTE and G. E. LUCAS, "Radiation Embrittlement of Nuclear Reactor Pressure Vessel Steel", ASTM Special Technical Publication/American Society for Testing and Materials, Philadelphia, PA, 909 (1986) p. 206.
13. J. T. BUSWELL, P. J. E. BISCHLER, S. T. FENTON, A. E. WARD and W. J. PHYTHIAN, *J. Nucl. Mater.* **205** (1993) 198.
14. E. A. LITTLE, *Int. Metall. Rev.* **204** (1976) 25.
15. J. F. STUBBINS, W.-J. SHONG, A. M. GIACOBBE, A. M. OUGOUAG and J. G. WILLIAMS, "Nuclear Reactor Vessel Thermal Annealing and Plant Life Extension", ASTM Special Technical Publication/American Society for Testing and Materials, Philadelphia, PA, 1204 (1993) p. 5.
16. M. K. DEVINE and D. C. JILES, *Rev. Prog. Quant. Non-Destruct. Eval.* **12** (1993) 1815.
17. B. D. CULLITY, "Introduction to magnetic materials" (Addison-Wesley, Reading, MA, 1972) p. 320.
18. L. B. SIPAHI, M. R. GORINDARAJU and D. C. JILES, *Rev. Prog. Quant. Non-Destruct. Eval.* **13** (1994) 1801.
19. J.-K. Yi, B.-W. LEE and H. C. KIM, *J. Magn. Magn. Mater.* **130** (1994) 81.
20. D. G. HWANG, H. C. KIM, *J. Phys. D.* **21** (1988) 1807.
21. B. L. EYRE and A. F. BARTLETT, *Phil. Mag.* **11** (1965) 53.
22. L. K. KEYS, J. P. SMITH and J. MOTEFF, *Phys. Rev.* **176** (1968) 851.

Received 11 April
and accepted 29 May 1997